Journal of the Korean Chemical Society
2017, *Vol. 61, No. 4*
Printed in the Republic of Korea
https://doi.org/10.5012/jkcs.2017.61.4.185

Facile Synthesis of CdTe Nanorods from the Growth of Te Nanorods

Weiwei Xu[†,‡], Jinzhong Niu[*,†], Shuang Zheng[†], Guimin Tian[†], Xinghui Wu[†], Yongguang Cheng[†], Xiaoyang Hu[†], Shuaishuai Liu[†], and Haoshan Hao[†]

[†]*College of Science, Henan Institute of Engineering, Zhengzhou, 451191, P. R. China*
[‡]*Key Laboratory for Special Functional Materials of Ministry of Education, Henan University, Kaifeng 475004, P. R. China*
[*]*E-mail: njz@haue.edu.cn*
(Received March 23, 2017; Accepted June 5, 2017)

ABSTRACT. One-dimensional CdTe nanorods (NRs) are obtained by the reaction of various Cd precursors with single crystalline Te nanorod templates, which are pre-synthesized from Te precursors by a simple and reproducible solvothermal method. Throughout the process, the diffraction intensity of different crystal facets of single crystalline Te NRs varied with reaction times. Finally, by alloying Cd ions along the axial direction of Te NRs, polycrystalline cubic phase CdTe NRs with diameters of 80–150 nm and length up to 1.2–2.4 μm are obtained. The nucleation and growth processes of Te and CdTe NRs are discussed in details, and their properties are characterized by XRD, SEM, TEM, Raman scattering, and UV-vis absorption spectra. It was found that the key elements of synthesizing CdTe NRs such as reaction temperatures and Cd sources will strongly influence the final shape of CdTe NRs.

Key words: Solvothermal method, Te, CdTe, Nanorods

INTRODUCTION

The synthesis and properties of one-dimensional (1D) semiconductor nanostructures, such as wires, rods and tubes, is an emerging research field for their various potential applications in electronics, photonics, life sciences, and nanodevices.[1–3] In particular, metal tellurides with a defined size and shape have attracted much attention due to the fundamental research to the effects of shape and size on physical and chemical properties.[4–6] In tellurium substances, Te atoms are believed to be bound together through van der Waals interactions in a hexagonal lattice and results a highly anisotropic crystal structure, thus leads to preferential formation of 1D structures, which had been demonstrated by many methods.[7–12] Different metal tellurides (Ag_2Te, $Cu_{2-X}Te$, Bi_2Te_3, CdTe) had been explored by using 1D Te nanostructures as templates.[13–17]

CdTe is of particular interest because it has a direct band gap energy of 1.44 eV, high absorption coefficient at room temperature and easy manufacturability. The synthesis techniques for CdTe have attracted people's interesting due to their unique properties.[18–22] For example, Zheng et al. developed an alternative approach for the synthesis of MSA-stabilized CdTe nanocrystals, in which Te NRs instead of unstable NaHTe were used as the Te source.[21] Nevertheless, to the best of our knowledge, further studies on the formation of CdTe nanowires by employing Te nanorods for solvothermal method and other key characteristics are still limited.

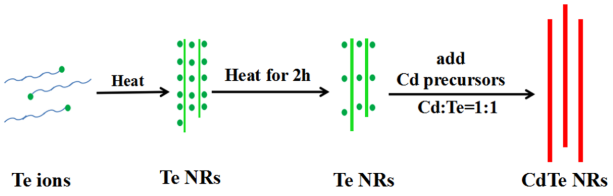

Scheme 1. Synthesis procedure for Te and CdTe NRs.

Herein, we report a friendly solvothermal method to synthesize CdTe NRs by using Te NRs as template in two stages (*Scheme* 1). In the first stage, Te NRs were synthesized from the Te precursor in three-necked bottle. Next, after the addition of the Cd precursor, Cd and Te were alloyed along the Te NRs in solution. The CdTe NRs were controlled by altering the experimental variables, such as the growth of Te NRs, reaction temperature, and Cd source. The properties of Te and CdTe NRs were investigated by detailed analysis from the experimental data.

EXPERIMENTAL

Chemicals

The materials used include cadmium acetate ($Cd(CH_3COO)_2$) (A.R.), sodium tellurite (Na_2TeO_3) (C.P.), ethylene glycol (EG) (A.R.), ethylenediamine (EN) (A.R.), polyvinylpyr-

rolidone (PVP) (A.R.), absolute ethanol (A.R.), 2,4-pentanedione (98%), triethylamine (99%), and $(C_2H_5)_2NCS_2Na\cdot 3H_2O$ (NaDDTC) were purchased from Tianjin Chemical Reagents Co. Ltd. All the chemicals were used as received without any further purification.

Synthesis of $Cd(acac)_2$

In a typical synthesis, 20 mmol $Cd(CH_3COO)_2$ was dissolved in 10 mL deionized water. Under magnetic stirring, 2,4-pentanedione (5 mL, 50 mmol) was added and kept stirring for 5 min. $Cd(acac)_2$ was precipitated after appropriate amount of triethylamine was added. Then, $Cd(acac)_2$ was washed for several times by ethanol and water, and finally was dried under room temperature.

Synthesis of $Cd(DDTC)_2$

In a typical synthesis, 0.05 mmol $Cd(CH_3COO)_2$ and 0.1 mmol NaDDTC was dissolved in 10 mL deionized water, respectively. Then, two solutions were mixed with stirring in a 100 mL beaker. After constant ambient condition for 3 h, the resulting yellow precipitate was filtered, washed with distilled water, and dried in air at 60 °C.

Synthesis of Te and CdTe NRs

In a typical synthesis of Te nanowires, 0.041 g of CH_3COONa, 0.056 g of Na_2TeO_3, and 0.200 g of PVP (molecular weight 30,000), 2.0 mL of EN and 10.5 mL of EG were put into 50 mL three-necked bottle under magnetic stirring. After vigorously stirring for 60 min at 40 °C, a clear solution was formed. The temperature was set at 175 °C under water reflux. During this process, the color of the reaction solution changed from colorless to black. After the reaction lasted for 2 h, Te NRs were formed. Then $Cd(acac)_2$ (0.25 mmol) ($Cd(CH_3COO)_2$ or $Cd(DDTC)_2$) was added and the reaction lasted for another 1 h, this resulted the formation of CdTe NRs. For purification, 50 mL of absolute ethanol was added and the unreacted compounds and byproducts were removed by centrifugation.

Characterization

X-ray diffraction (XRD) studies of NRs were carried out with a Bruker D8 advance X-ray diffractometer using Cu Kα radiation (wavelength = 0.154 nm). To get better signal-to-noise ratio, the XRD data were collected at a scan rate of 0.16 s with 0.02° per step. Transmission electron microscopy (TEM) studies were performed using a JEOL JEM-2100 electron microscope operating at 200 kV. Scanning electron microscopy (SEM) studies were performed using a FEI Quana-250 electron microscope operating at 15 kV. Raman spectra were acquired using a Renishaw inVia Reflex RAMAN Microscope equipped with a CW 532 nm HeNe laser. UV-vis absorption spectra were recorded using an UV-3600 spectrophotometer (Shimadzu Corporation). All optical measurements were performed at room temperature under ambient.

RESULTS AND DISCUSSION

Until now, a lot of preparation methods for Te NRs have been reported. Nevertheless, the use of autoclave and strong acid or strong alkali environment can't be avoided.[8,10,11,13,23] In our experiments, we chose three-necked bottle instead of the autoclave as reaction container, which can effectively avoid the long reaction time, and the product could be used readily as precursor to participate in subsequent reaction. The EG acts as both solvent and reducing agent in this case, and TeO_3^{2-} are reduced by EG to form elemental Te.[23–25]

Fig. 1 shows the typical SEM images of Te and CdTe NRs obtained under solvothermal conditions at 175 °C. Figure 1a and 1b show the morphology of Te NRs with diameters of 75–110 nm and lengths of 1–2 μm by the reaction time of 10 min and 120 min, respectively. It can be deduced that the rough Te NRs (10 min) are formed in a short time, and then, with the reaction continuing, Ostwald ripening determine the further growth of Te NRs. The small particles on the originally rough Te NRs gradually dissolve into the reaction solution and the concaves on the surface of Te NRs consequently are filled and more smooth NRs are formed. No obvious size change is observed for this

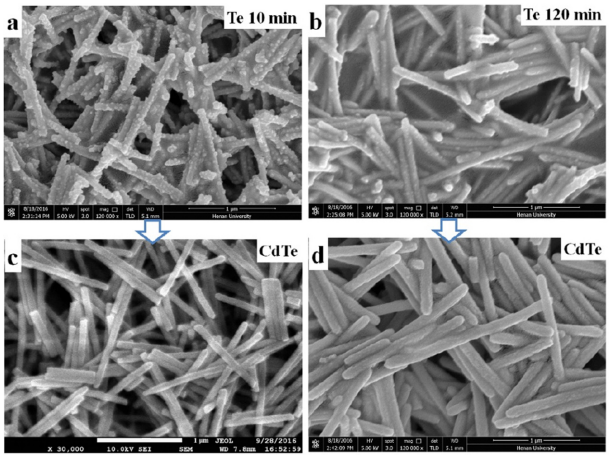

***Figure* 1.** SEM images of (a) Te NRs with the reaction time of 10 min; (b) Te NRs with the reaction time of 120 min; (c) CdTe NRs which were synthesized using Te NRs shown in *Fig.* 1a as template; (d) CdTe NRs which were synthesized using Te NRs shown in *Fig.* 1b as template.

rough Te (10 min) and smooth Te (120 min) NRs. After addition of Cd precursor, Cd ions react with the Te NRs promptly and CdTe NRs are formed. SEM images of CdTe NRs are shown in *Fig.* 1c and 1d. The width of CdTe NRs, which are synthesized by Te NRs prepared with 120 min of reaction as templates, is nearly 27 nm larger than the specimen which are synthesized by using Te NRs with 10 min of reaction (*Fig.* S1). During the reaction, the small particles on the Te NRs dissolve into the solution. However, under this situation, the Te ions in solution are almost unable to react with Cd ions in the solution to grow on the CdTe NRs. As a result, the CdTe NRs are smaller in diameter than the initial 10 min Te NRs.

Typical TEM images of Te and CdTe NRs are shown in *Fig.* 2. The morphologies of Te and CdTe NRs are similar to that shown in SEM images. For Te NRs, the small particles on the surface of Te NRs reduce significantly with reaction time, which can also be observed in TEM images. *Fig.* 2c shows that CdTe NRs have smooth surface without small particles on them. The HRTEM image of Te NR (*Fig*. 3a) indicates Te NR is single crystalline with the lattice spacings of 5.927 Å and 3.860 Å, corresponding to the lattice spacings of the (100) planes and (001) planes for trigonal structured tellurium, respectively. From the HRTEM image in the supporting information (*Fig*. S2), lattice spacing of the particles on the surface of Te NRs is 3.233 Å, corresponding to (111) planes of trigonal structured tellurium. *Fig*. 3b shows the lattice spacing is 3.742 Å for CdTe NRs, which is polycrystalline and corresponding to the (111) planes for cubic phase CdTe.

Based on the characterization results above, the nucleation and growth mechanisms of Te and CdTe NRs are discussed below. Due to the highly anisotropic crystal structure of Te, we can get one dimensional growth of Te NRs with high aspect ratios easily. The growth rate of Te atoms along the

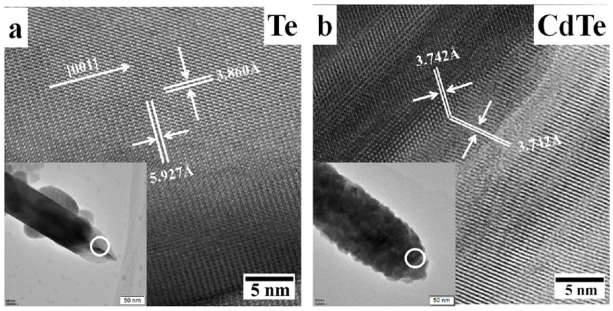

***Figure* 3.** HRTEM images of Te (a) and CdTe (b) NRs, which are corresponding to *Fig.* 2a and *Fig*. 2c, respectively.

axial direction is faster than that along the radial direction in the early stage of nucleation, and this induces the 1D growth along the c-axis.[26–30] With reaction lasting, the size of Te NRs has no obvious change and the particles on the surface of Te NRs disappear in the annealing process. After addition of Cd precursor, due to the diffusion of atoms by their supersaturation in the solution, the formation of CdTe NRs develops fast. Heterogeneous nucleation occurs on Te NRs everywhere and generates CdTe polycrystallines in the rods.[17] The morphology of CdTe NRs is determined by the pre-synthesized Te NRs. If Cd and Te precursors are loaded at the same time in the reaction, the morphology of product is uncontrolled (*Fig*. S3 in supporting information).

Fig. 4a represents typical XRD patterns of as synthesized Te and CdTe NRs. All of the peaks in the XRD pattern of Te NRs (*Fig*. 4a) can be perfectly indexed to the trigonal phase of tellurium, which are consistent with the reported XRD data (JCPDS no. 36-1452). But, the relative peak intensities change when the reaction time progress from 10 min to 120 min, which further confirm the reduction of the small particles on the surface of Te NRs. After addition of Cd precursor, CdTe NRs are synthesized. The diffraction pattern is consistent with the cubic phase struc-

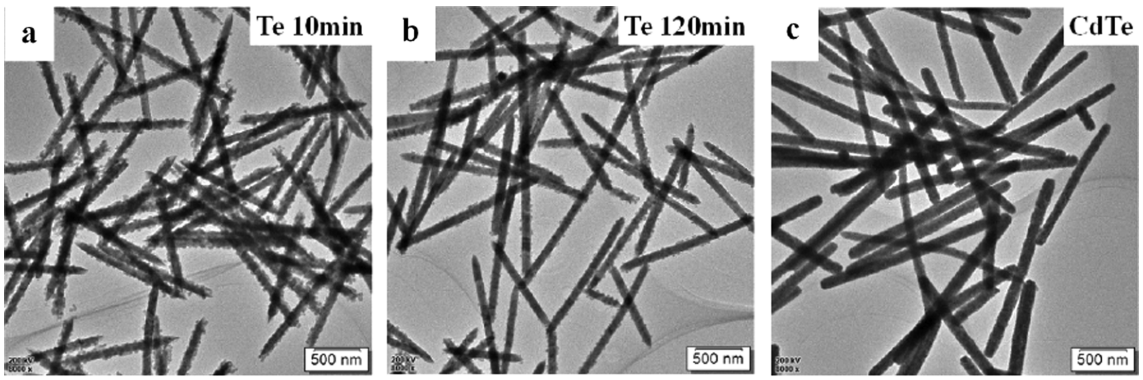

***Figure* 2.** TEM images of Te NRs (a), Te NRs (b), and CdTe NRs (c), which are corresponding to *Fig*. 1a, *Fig*. 1b, and *Fig.* 1d, respectively.

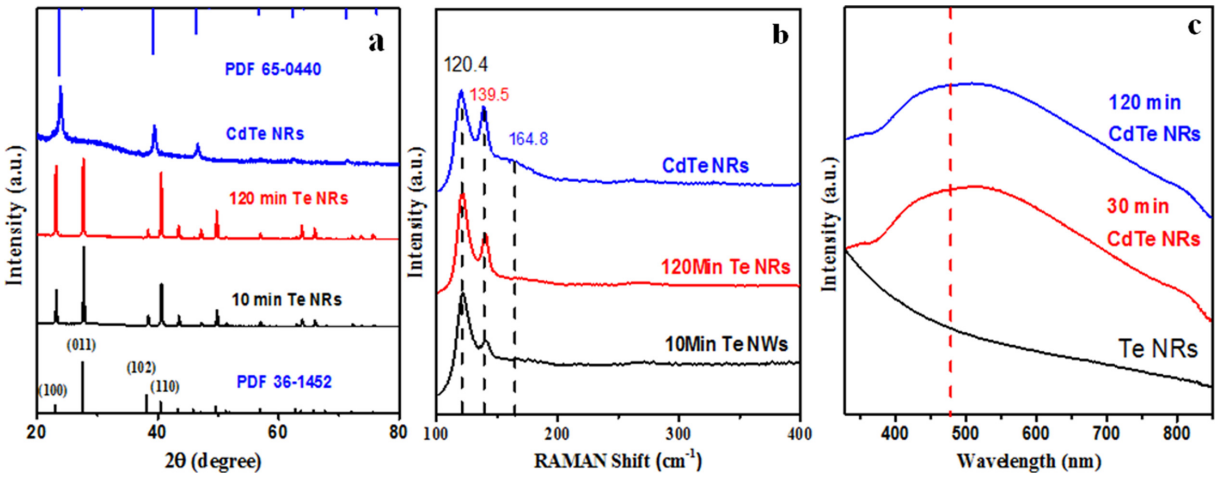

***Figure* 4.** XRD (a), Raman (b), and UV-vis absorption (c) spectra of Te and CdTe NRs.

ture (JCPDS no. 65-0440). The crystal sizes of CdTe NRs are 26 nm, 23 nm, and 20 nm calculated by Scherrer equation according to the crystal facet of (110), (220) and (311), respectively. This result further prove the polycrystalline structure of CdTe NRs, which is consistent with the result of HRTEM characterizations.

Raman spectra of Te and CdTe NRs (*Fig.* 4b) are recorded to evaluate the structural change that might occur to the Te NRs. For Te NRs, there are two Raman peaks locate at 120.4 and 139.5 cm^{-1}, which are attributed to A1(Te) and E(Te), respectively.[31,32] The appearance of an intense A1 band indicates the high crystalline quality of the Te NRs. The relative intensity of E(Te) peak increases with the proceeding of reaction, which may be attribute to the completion of growth of Te crystals. Generally, the presence of modes about Te is usually observed in CdTe samples. For CdTe NRs, there are three Raman peaks at 120.4, 139.5, and 164.8 cm^{-1}, which are attributed to A1(Te), E(Te) or TO(CdTe) mode, and LO modes of CdTe, respectively.[32,33] These phonon peaks indicated the high quality of CdTe NRs.

The formation of CdTe NRs also is demonstrated by the absorption peaks in the UV–vis spectra. *Fig.* 4c represents a change in the absorption spectra of Te and CdTe NRs. For Te NRs, there is no obvious characteristic absorption peak in the visible light region. After addition of Cd precursors, the absorption peak appears at 480 nm, which is attributed to the generation of CdTe. This observation is consistent with the TEM images and XRD results.

It is found that the reaction temperature could also significantly influence the reaction kinetics and the obtained products. SEM image and XRD pattern of the reaction products synthesized at different temperatures with all the other reaction conditions unchanged are shown in *Fig.* 5.

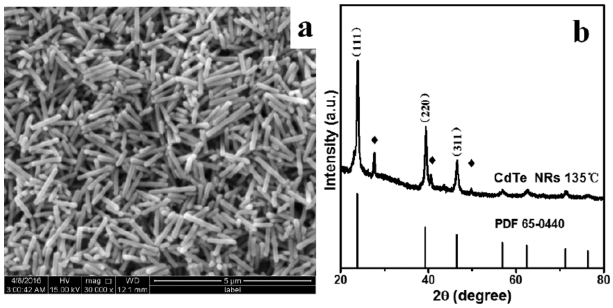

***Figure* 5.** SEM image and XRD pattern of CdTe NRs which were synthesized at 135 °C.

When the reaction temperature is higher than 175 °C, reaction solution became boiling, which leads to the reaction uncontrolled. When the reaction temperature is set to 135 °C, the morphology of CdTe NRs is similar with CdTe NRs synthesized at 175 °C. But, the XRD result proves that the product has both Te (PDF 36-1452) and CdTe (PDF 65-0040) phases. It is obvious that the reaction temperature influences the reaction product and higher temperature favors the quick growth and complete formation of CdTe NRs.

Besides the reaction temperature, it is found that the Cd precursors could also significantly influence the products. In our control experiments, $Cd(CH_3COO)_2$ and $Cd(DDTC)_2$ have also been used as common Cd precursors. When $Cd(CH_3COO)_2$ is used as Cd precursor, the morphology of obtained CdTe NRs (*Fig.* 6a) is similar with the products when use $Cd(acac)_2$ (*Fig.* 1d) as Cd precursor. However, the XRD pattern shows that relative peak intensity is changed. For the use of $Cd(CH_3COO)_2$, the crystal face intensity of (111):(200):(311) for CdTe NRs is weaker than the use of $Cd(acac)_2$. For the use of $Cd(DDTC)_2$ as Cd precursors,

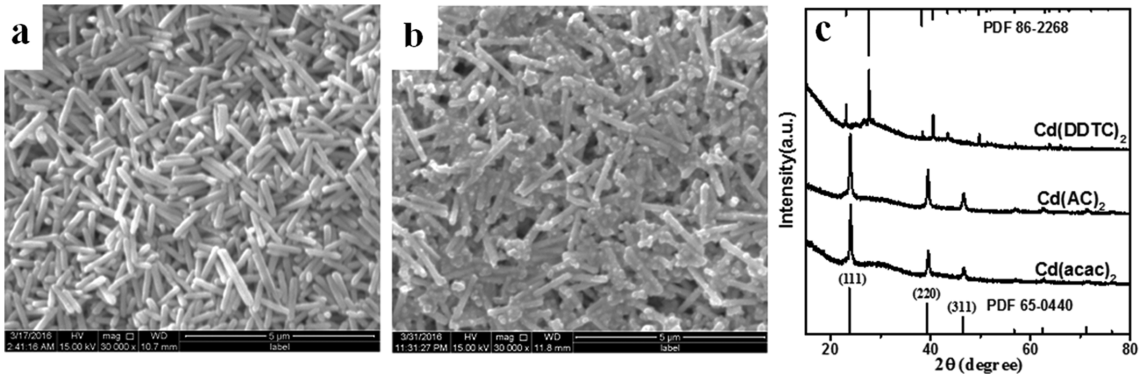

***Figure* 6.** SEM images of CdTe NRs which were synthesized by using (a) $Cd(CH3COO)_2$ and (b) $Cd(DDTC)_2$ as Cd precursor, (c) XRD patterns of CdTe NRs, which are corresponding to *Fig.* 6a, *Fig.* 1d, and *Fig.* 6b, respectively.

the morphology of product is uncontrollable as shown in *Fig.* 6b, and XRD pattern in *Fig.* 6c shows the mixture phase for Te (JCPDS no. 36-1452) and CdTe (JCPDS no. 65-0440). It is obvious that $Cd(DDTC)_2$ precursor is unsuitable under this experiment condition, and $Cd(CH_3COO)_2$ is another choice for the preparation of CdTe NRs by this convenient solvothermal route.

CONCLUSION

Te and CdTe NRs have been successfully synthesized by a convenient solvothermal route. The proposed synthesis method is simple and reproducible. The nucleation and growth of Te and CdTe NRs are supposed and proved by the results. The results indicate that CdTe NRs are polycrystalline with cubic phase and have high crystallinity by using pre-synthesized single crystalline Te NRs as templates. In addition, this simple method does not need the subsequent complicated workup procedures such as the removal of the template, and avoid the use of the autoclave, which shows the potential in the future applications for the preparation of CdTe based solar cells.

Acknowledgments. This study was funded by the program for key scientific research projects in colleges and universities of Henan province (grant number 16A140026) and doctor fund of Henan Institute of Engineering (grant number D2014005 and D2012019).

REFERENCES

1. Duan, X.; Huang, Y.; Cui, Y.; Wang, J.; Lieber, C. M. *Nature* **2001**, *409*, 66.
2. Manzoor, U.; Kim, D. K. *Scripta Mater.* **2006**, *54*, 807.
3. Utama, M. I.; Zhang, J.; Chen, R.; Xu, X.; Li, D.; Sun, H.; Xiong, Q. *Nanoscale* **2012**, *4*, 1422.
4. Gur, I.; Fromer, N. A.; Geier, M. L.; Alivisatos, A. P. *Science* **2005**, *310*, 462.
5. Yang, J.; Gao, Y.; Kim, J. W.; He, Y.; Song, R.; Ahn, C. W.; Tang, Z. *Phys. Chem. Chem. Phys.* **2010**, *12*, 11900.
6. You, H.S.; Choi K. S.; Bae P. K.; Kim, K. N.; Jang, H. G.; Kim Y.; Kim C. H. *Bull. Korean Chem. Soc.* **2009**, 30, 3137.
7. Lin, Z. H.; Yang, Z.; Chang, H. T. *Cryst. Growth Des.* **2008**, *8*, 351.
8. Gautam, U. K.; Rao, C. N. R. *J. Mater. Chem.* **2004**, *14*, 2530.
9. Xi, G.; Liu, Y.; Wang, X.; Liu, X.; Yiya Peng, A.; Qian, Y. *Crys. Growth Des.* **2006**, *6*, 2567.
10. Wu, X. P.; Yuan, L.; Zhou, S. M.; Lou, S. Y.; Wang, Y. Q.; Gao, T.; Liu, Y. B.; Shi, X. J. *J. Nanopart. Res.* **2012**, *14*, 721.
11. Wu, X.; Wang, Y.; Zhou, S.; Gao, T.; Wang, K.; Lou, S.; Liu, Y.; Shi, X. *Cryst. Growth Des.* **2012**, *13*, 136.
12. Narayanan, R.; Sarkar, D.; Som, A.; Wleklinski, M. S.; Cooks, R. G.; Pradeep, T. *Anal. Chem.* **2015**, *87*, 10792.
13. Dong, G. H.; Zhu, Y. J.; Cheng, G. F.; Ruan, Y. J. *Mater. Lett.* **2012**, *76*, 69.
14. Zhou, C.; Dun, C.; Wang, Q.; Wang, K.; Shi, Z.; Carroll, D. L.; Liu, G.; Qiao, G. *ACS Appl. Mat. Interfaces* **2015**, *7*, 21015.
15. Bhatt, R.; Krishnan, G.; Bhattacharya, S.; Bohra, A.; Bhatt, P.; Basu, R.; Singh, A.; Aswal, D. K.; Gupta, S. K. *Aip Conference Proceedings* **2016**, *1731*, 4261.
16. Ananthakumar, S.; Ramkumar, J.; Babu, S. M. *Mater. Sci. in Semicond. Process.* **2014**, *27*, 12.
17. Kim, S. H.; Kim, J. J.; Suh, S. W.; Park, B. K.; Lee, J. B. *J. Ind. Eng. Chem.* **2010**, *16*, 741.
18. Shen, H.; Wang, H.; Chen, X.; Niu, J. Z.; Xu, W.; Li, X. M.; Jiang, X. D.; Du, Z.; Li, L. S. *Chem. Mater.* **2010**, *22*, 4756.
19. Hwang, C. H.; Park, J.; Song, M.; Lee, J.; Shim, I. *Bull. Korean Chem. Soc.* **2011**, 32, 2207.
20. Hou, T. C.; Yang, Y.; Lin, Z. H.; Ding, Y.; Chan, P.; Pradel,

K. C.; Chen, L. J.; Wang, Z. L. *Nano Energy* **2013**, *2*, 387.
21. Zheng, R.; Guo, S.; Dong, S. *Inorg. Chem.* **2007**, *46*, 6920.
22. Yong, S. M.; Muralidharan, P.; Jo, S. H.; Kim, D. K. *Mater. Lett.* **2010**, *64*, 1551.
23. Zhang, L.; Yang, H.; Yu, J.; Shao, F.; Li, L.; Zhang, F.; Zhao, H. *J. Phys. Chem. C* **2009**, *113*, 5434.
24. Wang, J.; Wang, X.; Peng, Q.; Li, Y. *Inorg. Chem.* **2004**, *43*, 7552.
25. Sun Y.; Yin Y.; Mayers B. T.; Herricks T.; Xia Y. *Chem. Mater.* **2002**, *14*, 4736.
26. Mayers, B.; Xia, Y. *J. Mater. Chem.* **2002**, *12*, 1875.
27. Mayers, B.; Xia, Y. *Adv. Mater.* **2002**, *14*, 279.
28. Wei, G.; Deng, Y.; Lin, Y. H.; Nan, C. W. *Chem. Phy. Lett.* **2003**, *372*, 590.
29. Lu, Q.; Gao, F.; Komarneni, S. *Adv. Mater.* **2004**, *16*, 1629.
30. Zhu, Y. J.; Wang, W. W.; Qi, R. J.; Hu, X. L. *Angew. Chem. Int. Ed.* **2004**, *43*, 1410.
31. Yan, C.; Raghavan, C. M.; Kang, D. J. *Mater. Lett.* **2014**, *116*, 341.
32. Mak, J. S. W.; Farah, A. A.; Chen, F.; Helmy, A. S. *Acs Nano* **2011**, *5*, 3823.
33. Ma, L.; Wei, Z.; Zhang, F.; Wu, X. *Superlattices Microstruct.* **2015**, *88*, 536.